

Supplementary Information

pH Dependent Isotropic to Nematic Phase Transitions in Graphene Oxide Dispersions Reveal Droplet Liquid Crystalline Phases

Rachel Tkacz^a, Rudolf Oldenbourg^b, Shalin B. Mehta^b, Morteza Miansari^a, Amitabh Verma^b,
Mainak Majumder^{*a}

^a Nanoscale Science and Engineering Laboratory (NSEL) and Mechanical and Aerospace Engineering Department, Monash University, Clayton, VIC 3800, Australia

^b Marine Biological Laboratories, Woods Hole MA 02543, and Physics Department, Brown University, Providence RI 02912, USA.

*Email: mainak.majumder@monash.edu; Tel: +61399056255

Section S1: GO synthesis:

GO was synthesized from graphite powder (SP-1 grade 325 mesh, Bay Carbon Inc.) using a modified hummers method.^{1,2} 10 g of graphite powder was added to a pre-treatment solution for approximately 30 minutes. The pre-treatment solution was prepared by adding 50 ml of heated (90 °C) concentrated H₂SO₄ to a 300 ml beaker with 5 g of K₂S₂O₈ and 5 g of P₂O₅ and stirred till completely dissolved and cooled to 80°C. The mixture of this solution and the graphite was then kept at 80°C for 4.5h and then diluted with 1 L of DI water and left overnight. The next day the product was filtered over a 0.22 µm pore size nylon membrane and washed with water. The solid residue was allowed to air dry overnight. The oxidation of the graphite was done by placing 230 ml of H₂SO₄ into a 2 L Erlenmeyer flask and cooling it to 0 °C in an ice bath. The pre-treated graphite was then added to the acid slowly with stirring along with 30 g of KMnO₄ while the temperature was maintained below 10 °C. The solution was then allowed to react at 35 °C for 2 h after which 460 ml of DI water was added in 20-30 ml aliquots, in an ice bath while the temperature is kept below 50 °C. The mixture changes colour to brown as it reacts. The mixture was stirred for 2 h after which 1.4L of DI water was added, followed by 25 ml of 30% H₂O₂ resulting in a yellow colour with bubbling. The mixture allowed to settle for at least 24 h after which the clear supernatant was decanted. The remaining material was centrifuged and washed with 2.5 L of 10% HCl solution followed by 2.5 L DI water. To prepare a GO suspension some of the above product was diluted with Millipore water to a required concentration and sonicated using UP-100 Ultrasonic processor from E-Chrom Tech.

Section S2: GO suspensions at pHs 1 and 14:

At pHs 1 and 14 the GO suspensions did not form liquid crystals due to aggregation. At pH 1 the aggregates had fine texture that could only be detected by the optical microscope, while at pH 14 an immediate aggregation and darkening of suspension was observed by a naked eye. The reason for aggregation in the low pH 1 is probably an excess of electrolyte, which cause to screening of the electrostatic double layer and decrease the suspension stability³. The aggregation at pH 14 is probably due to both excess of electrolyte and rapid reduction of the GO by the high concentration of NaOH, as was shown before^{4, 5} and by darkening of the suspension (also UV-vis spectrometry for pH 9 in Figure S3 in section S4 supports the reduction).

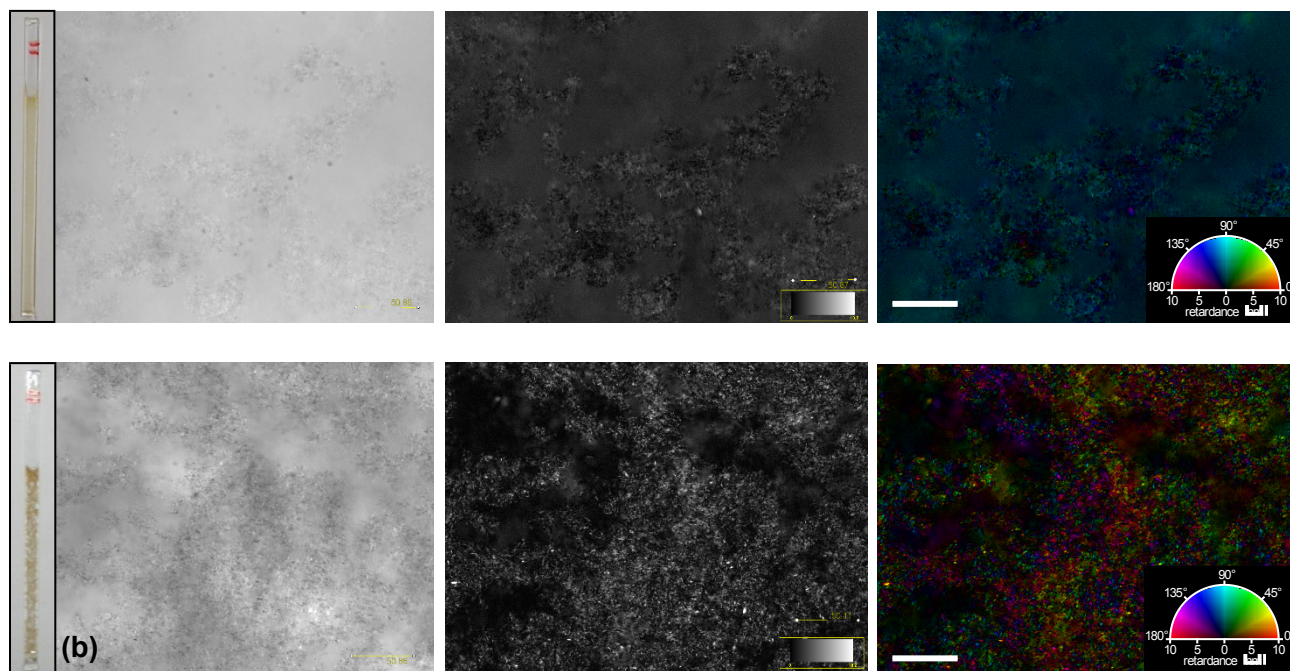


Figure S1: LC-PolScope images of a 1 mg/ml GO suspension at pHs 1 (a) and 14 (b). Scale bar is 50 μm . Polarized light images (left) and the cross-polar processed images of the retardance represented by brightness (center, retardance scale bars are 0-10 nm) and the retardance and azimuth display (right), in which brightness represents the apparent retardance and hue the azimuth (retardance scale bars are 0-10 nm). In the insets: the capillary tubes with the aggregates.

Section S3: GO liquid crystals at pH 9:

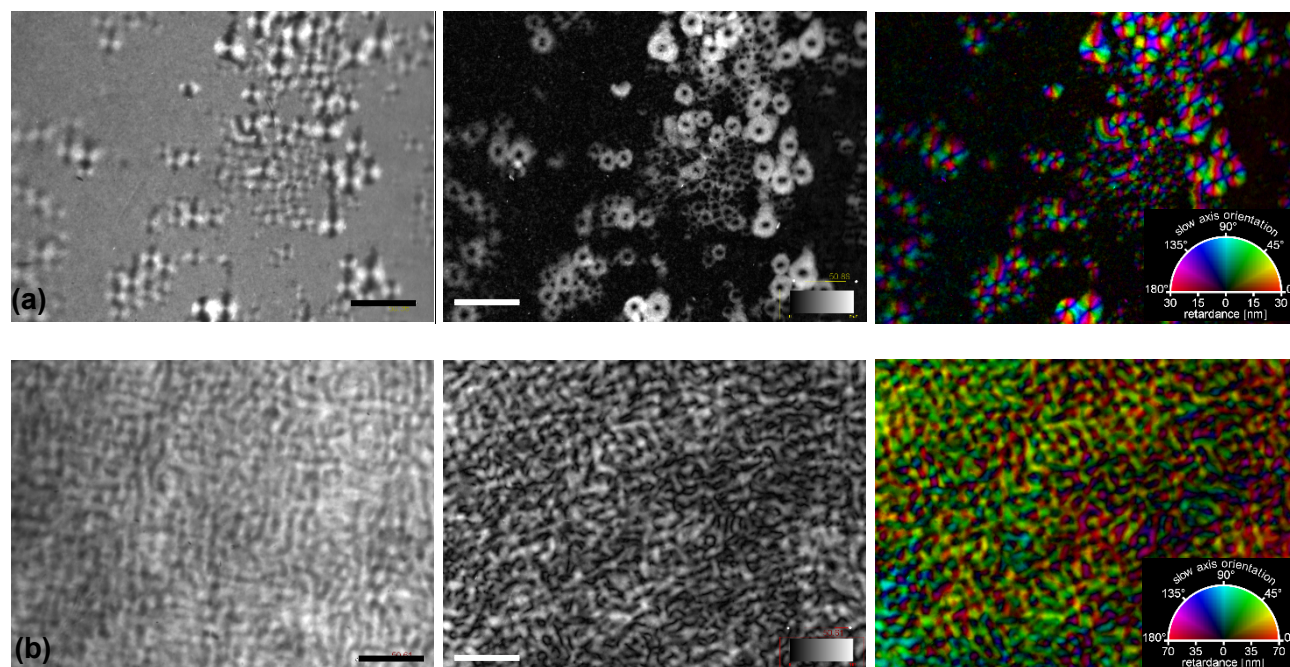


Figure S2: LC-PolScope images of a 9 mg/ml GO suspension at pH 9 in the bi-phasic (a) displays spherical domains, which later accumulate at the bottom of the capillary tube to form nematic phase with worm-like texture (b). Scale bar is 50 μm . One of the raw images recorded using elliptically polarized light (left) and the cross-polar processed images of the retardance represented by brightness (center, retardance scale bars are 0-30 nm for (a) and 0-70 nm for (b)) and the retardance and azimuth display (right), in which brightness represents the apparent retardance and hue the azimuth.

Section S4: A qualitative illustration of the surface charge density of large and small GO sheets at different pH values:

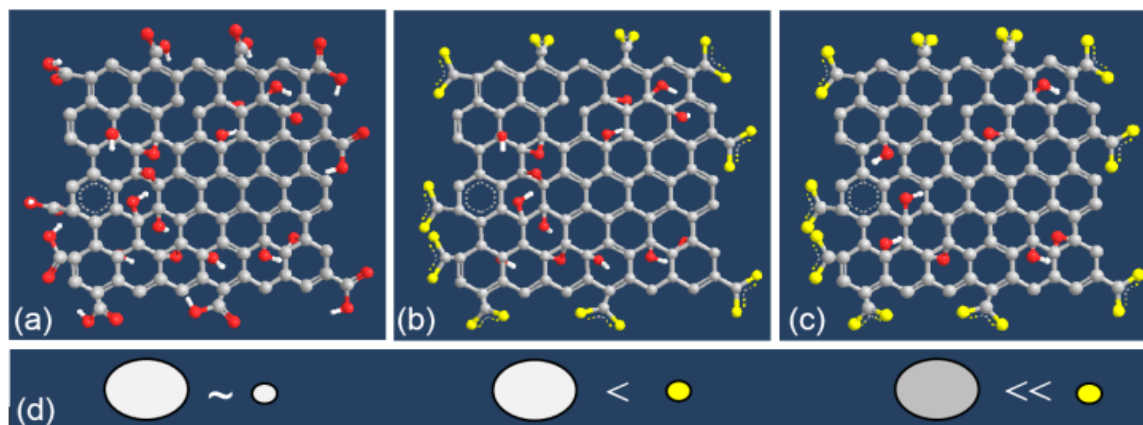


Figure S3: Schematic illustration of the size-based surface charge density of GO sheets as a function of pH. (a-c) GO structure and oxidative states at pHs 2 (a), 6 (b) and 9 (c); carbons atoms in grey, un-charged oxygens in red, charged oxygens in yellow and hydrogens in white. (d) Qualitative comparison between the surface charge density of large GO sheets and small ones for pH 2 (left), 6 (center) and 9 (right).

Section S5: UV-vis spectra of GO suspensions at different pH values:

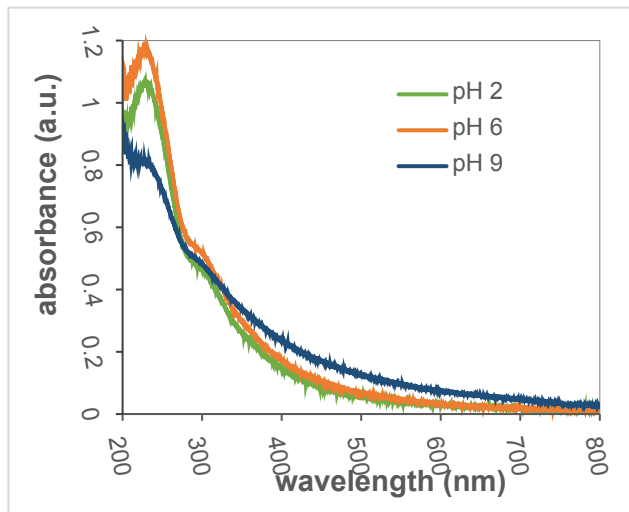


Figure S4: UV-vis spectra of GO at different pH values formed by addition of HCl or NaOH, and after remaining for few days at those conditions.

Section S6: Quantitative analysis of dimensions of GO sheets:

The dimension of GO sheets was estimated by performing quantitative analysis on SEM images using ImageJ. The average diameter of each sheet was calculated assuming a disk-like shape, and the average of at least 500 sheets for each phase was taken for these studies. SEM samples were prepared by dip-coating of silicon wafers with 0.01 mg/ml GO suspensions. We used a Nova NanoSEM™ 450, FEI, Hillsboro, OR instrument, and imaged at 3kV. Typical SEM images for the isotropic and nematic phases at pH 6 are shown in Figure S5.

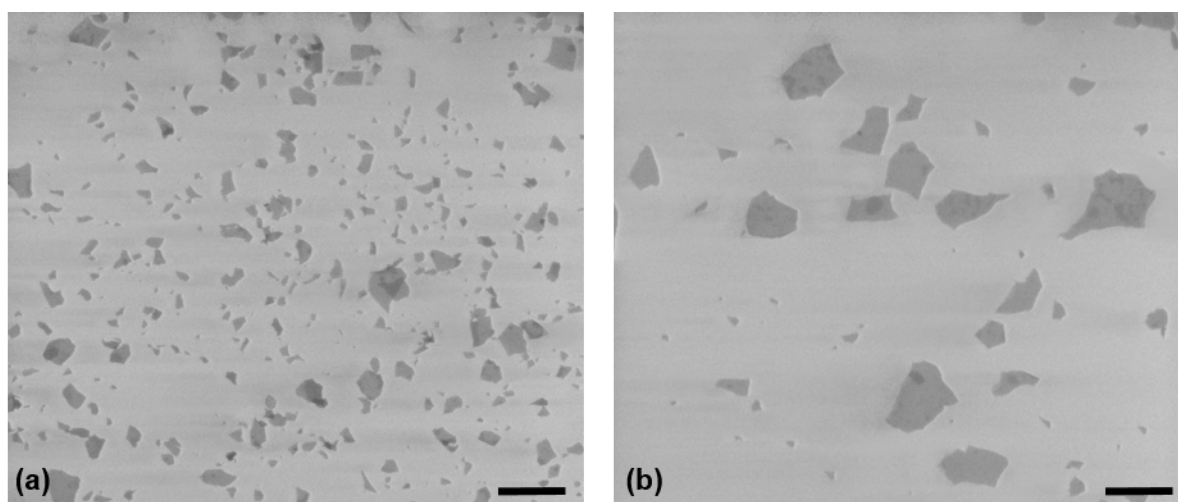


Figure S5: Typical SEM images of GO sheets from the isotropic (a) and the nematic (b) phases at pH 6 (scale bar is 2 μm) showing that the nematic phase has been enriched with larger GO sheets.

Section S7: The merging process of spherical domains to a ‘worm-like’ nematic phase at pHs > pKa:

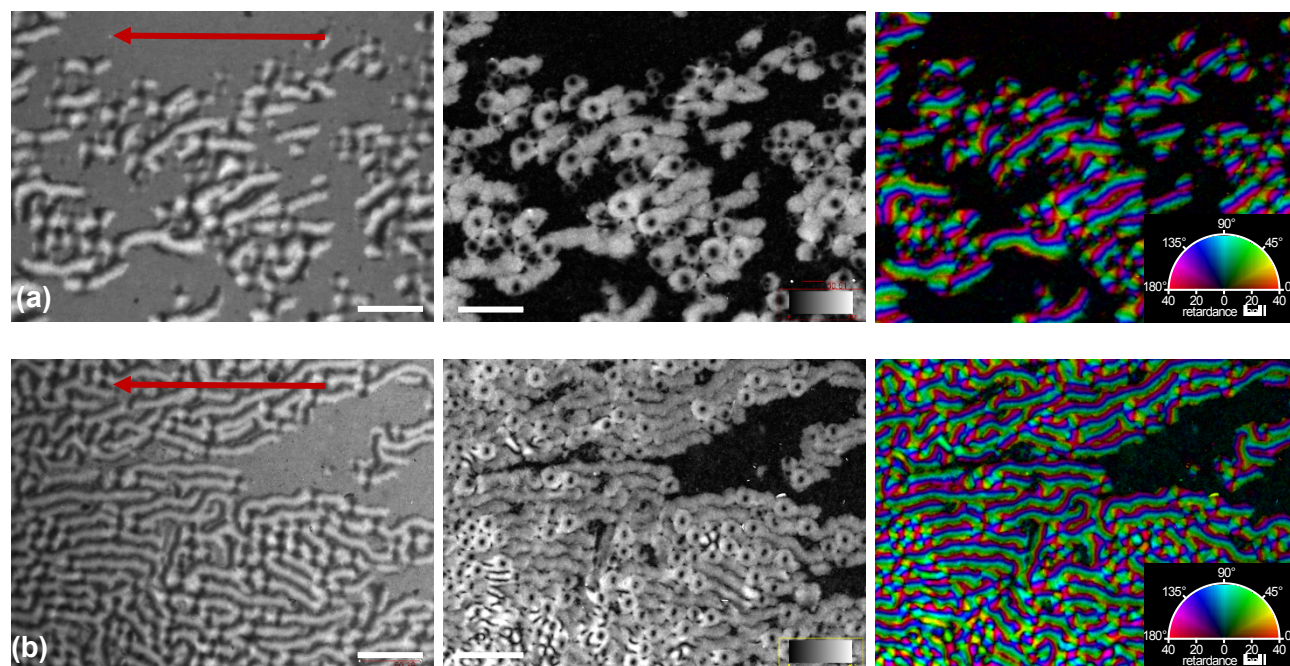


Figure S6: LC-PolScope images of the merging of nematic droplets to a worm-like nematic phase at the bottom of capillary tube, in a 9 mg/ml GO suspension at pHs 6 (a) and 9 (b). The red arrows show the direction of movement. Scale bar is 50 μm . One of the raw images recorded using elliptically polarized light (left) and the cross-polar processed images of the retardance represented by brightness (center, retardance scale bar is 0-40 nm) and the retardance and azimuth display (right), in which brightness represents the apparent retardance and hue the azimuth.

Section S8: Tracking the phase-separation (I-N) process with time:

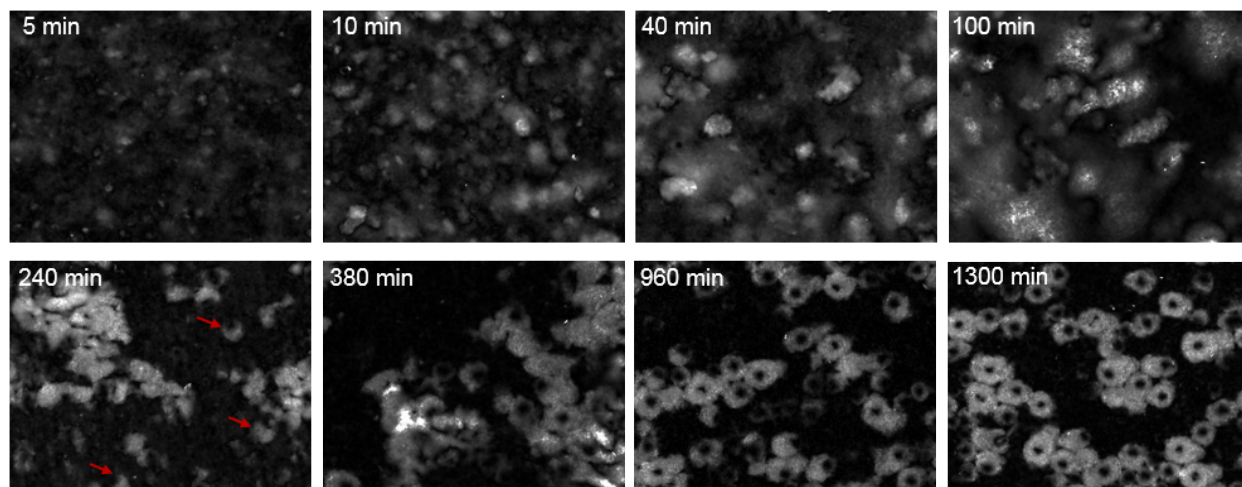


Figure S7: Time-lapse apparent retardance images of the formation of spherical GO liquid crystal domains from a 9mg/ml isotropic suspension at pH 6. Phase separation of nematic domains from the isotropic one can be seen in the top row, and annealing of the internal structure of the droplets to tangential alignment of the GO sheets can be seen in the bottom row. The arrows at 240 min are pointing to domains that start to show this process.

Section S9: Eliminating the possibility of anchoring around a gas bubble:

In order to eliminate the possibility of the formation of the spherical shape due to anchoring around a gas bubble (air or water vapors), which might have resulted by trapped bubbles from the sonication procedure, we prepared a GO suspension at pH 6 with no sonication at all. To give the suspension some homogeneity we stirred the Ependorf for 1 hour in a vortex stirrer, keeping in mind that this method is far from being optimized for creation of homogenous GO dispersion. Spherical droplets were obtained and are shown by the apparent retardance in Figure S6. The shape of the spheres is slightly less uniform probably due to the lack of uniformity in the starting suspension. However, this result clearly demonstrates that the sonication has no influence on the droplet formation, but on homogenizing the suspensions only.

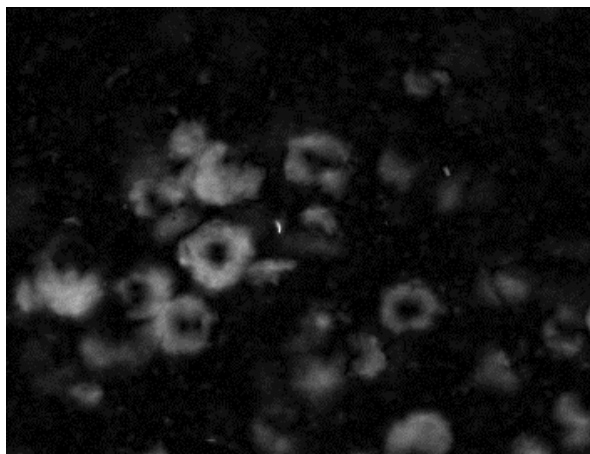


Figure S8: The apparent retardance of GO liquid crystals formed in suspension that was not exposed to ultrasonication, at pH 6.

1. N. I. Kovtyukhova, P. J. Ollivier, B. R. Martin, T. E. Mallouk, S. A. Chizhik, E. V. Buzaneva and A. D. Gorchinskiy, *Chem. Mater.*, 1999, **11**, 771-778.
2. W. S. Hummers and R. E. Offeman, *J. Am. Chem. Soc.*, 1958, **80**, 1339-1339.
3. J. N. Israelachvili, *Intermolecular and Surface Forces* 3edn., Elsevier Inc, 2011.
4. X. Fan, W. Peng, Y. Li, X. Li, S. Wang, G. Zhang and F. Zhang, *Adv. Mater. (Weinheim, Ger.)*, 2008, **20**, 4490-4493.
5. S. D. Perera, R. G. Mariano, N. Nijem, Y. Chabal, J. P. Ferraris and K. J. Balkus Jr, *J. Power Sources*, 2012, **215**, 1-10.